END
DATE
FILMED

9 -77

DDC

1.0

1.1

1.25   1.4   1.6

2.8   2.5

3.2   2.2

3.6

4.0   2.0

1.8

DNA 4209F

A METHOD OF PRELIMINARY DESIGN ANALYSIS FOR NORMAL IMPACT OF EARTH PENETRATORS

Georgia Institute of Technology

Georgia Tech Research Institute

Atlanta, Georgia 30332

February 1977

Final Report for Period 30 October 1975—31 March 1977

CONTRACT No. DNA 001-76-C-0166

APPROVED FOR PUBLIC RELEASE;
DISTRIBUTION UNLIMITED.

Prepared for

Director

DEFENSE NUCLEAR AGENCY

Washington, D. C. 20305

D D C

RECEIVED

SEP 1 1977

B

Destroy this report when it is no longer
needed. Do not return to sender.

REPORT DOCUMENTATION PAGE		READ INSTRUCTIONS BEFORE COMPLETING FORM
1. REPORT NUMBER DNA 4209F	2. GOVT ACCESSION NO.	3. RECIPIENT'S CATALOG NUMBER
4. TITLE (and Subtitle) A METHOD OF PRELIMINARY DESIGN ANALYSIS FOR NORMAL IMPACT OF EARTH PENETRATORS.		5. TYPE OF REPORT & PERIOD COVERED Final Report for Period 30 Oct 75 — 31 Mar 77
		6. PERFORMING ORG. REPORT NUMBER
7. AUTHOR(s) L. W. Rehfield S. V. Hanagud		8. CONTRACT OR GRANT NUMBER(s) DNA 001-76-C-0166
9. PERFORMING ORGANIZATION NAME AND ADDRESS Georgia Institute of Technology Georgia Tech Research Institute Atlanta, Georgia 30332		10. PROGRAM ELEMENT, PROJECT, TASK AREA & WORK UNIT NUMBERS NWED Subtask Y99QAXSB048-17
11. CONTROLLING OFFICE NAME AND ADDRESS Director Defense Nuclear Agency Washington, D.C. 20305		12. REPORT DATE February 1977
		13. NUMBER OF PAGES 46
14. MONITORING AGENCY NAME & ADDRESS(if different from Controlling Office)		15. SECURITY CLASS. (of this report) UNCLASSIFIED
		15a. DECLASSIFICATION DOWNGRADING SCHEDULE

16. DISTRIBUTION STATEMENT (of this Report)

Approved for public release; distribution unlimited.

17. DISTRIBUTION STATEMENT (of the abstract entered in Block 20, if different from Report)

19. KEY WORDS (Continue on reverse side if necessary and identify by block number)

Earth Penetration
Projectile Penetration
Structural Dynamic Modeling
Terradynamics

20. ABSTRACT (Continue on reverse side if necessary and identify by block number)

A simplified method of analysis for use in preliminary design of earth penetrators has been developed. The objectives have been simplicity, rapid turnaround and low cost, in addition to sufficient accuracy for adequate prediction of primary physical processes and associated variables. Based upon a stress wave transmission approach, the method applies to axisymmetric response of projectiles of revolution due to normal impact events in its current state of development. Results are presented for strain and acceleration time histories on a penetrator that has been impact tested. NEXT PAGE

DD FORM 1473 EDITION OF 1 NOV 65 IS OBSOLETE
1 JAN 73

403 914

20. ABSTRACT (Continued)

Analysis predictions and available experimental data are in excellent agreement, which indicates that the method is effective as well as efficient.

PREFACE

This report describes the development and application of
a method of analysis suitable for preliminary design of earth
penetrators. Only normal impact events are considered. The work
was performed by the School of Aerospace Engineering, Georgia
Institute of Technology. Professor L. W. Rehfield served as
Project Director and Co-Principal Investigator. Professor S. V.
Hanagud was the other Co-Principal Investigator.

The Project Officer was Major David R. Spangler, SPSS, Defense
Nuclear Agency.

ACCESSION for

NTIS	White Section	☑
DDC	Buff Section	☐
UNANNOUNCED		☐
JUSTIFICATION		

BY
DISTRIBUTION/AVAILABILITY CODES

Dist.	Avail. and/or SPECIAL	
A		

1

CONTENTS

INTRODUCTION

Overview

The work described herein is part of a larger program sponsored
by the Defense Nuclear Agency to develop the base for earth penetration
technology. The objectives of the overall program are to assess the
state-of-the-art in design analysis prediction techniques for realistic
earth penetrating vehicles (EPV's) and to establish a groundwork of
experimental data obtained under controlled conditions. Several parallel
analytical prediction studies have been undertaken, along with two well-
instrumented penetration tests.

The tests have been performed by the Avco Corporation in so-called
reverse ballistic fashion.* Two normal impact events were staged for
sandstone target material and approximately 1800 feet per second impact
velocity. The penetrators used in the tests were designed and built
by the Sandia Corporation[1] for reverse ballistic testing; they are half
scale and shown in Figure 1.** The penetrators were thoroughly instrumented
with 36 strain gages and 5 accelerometers installed at locations that
were both important and accessible.[2] The data taken is currently avail-
able in preliminary form as Reference 3.

A simplified method of analysis for use in preliminary design of
EPV's is described herein. In addition, strain and time history predic-
tions for key locations on the primary structure obtained by this method are

---

*This type of test is conducted with a stationary penetrator and
a moving target block.

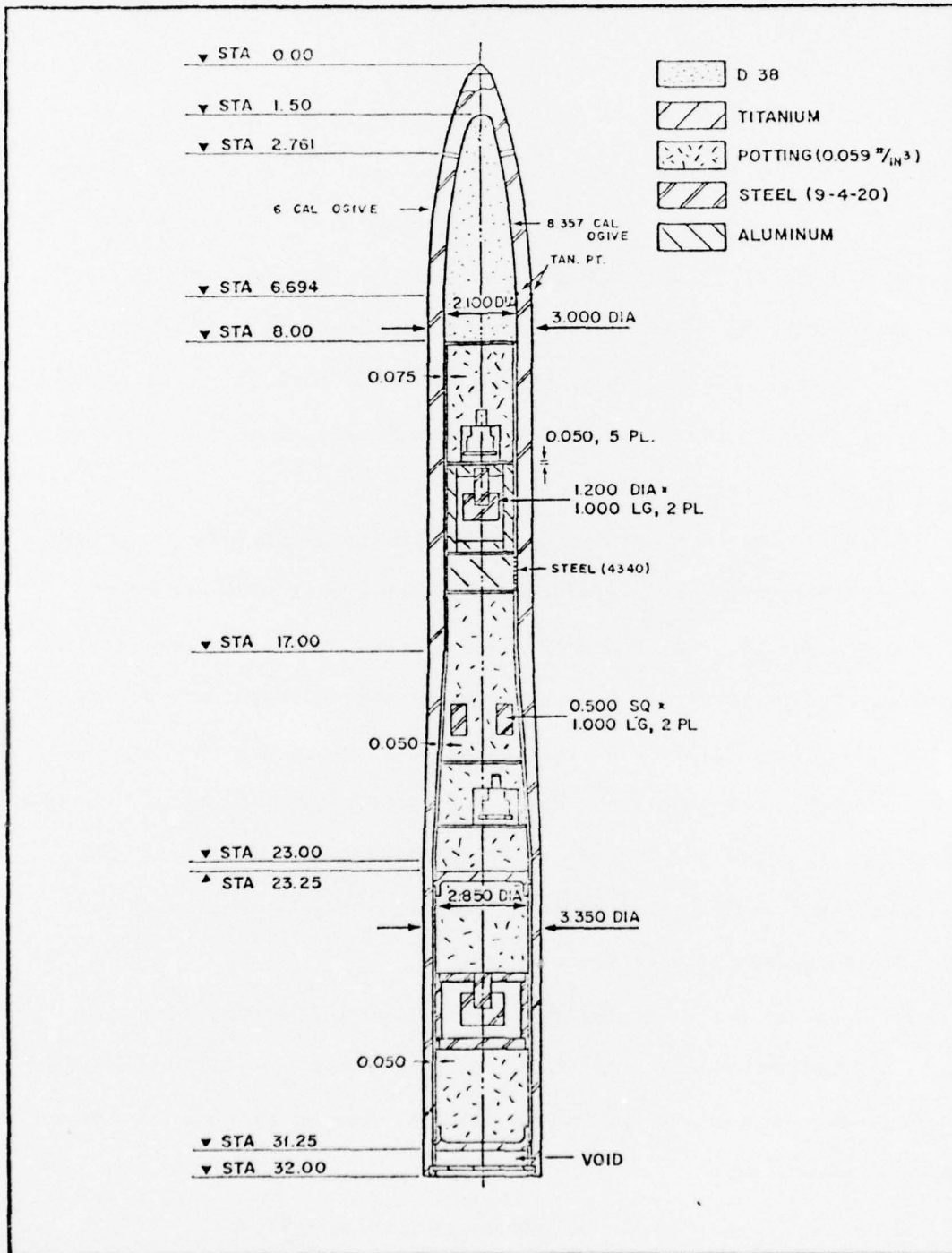**In the sequel, we will refer to these simply as the "penetrators".

3

Figure 1. DNA Half Scale Penetrator

are presented for comparison with the penetrator tests.[3] The predictions are obtained from simple closed form analytical expressions and are in excellent agreement with available experimental data. This indicates that the method of analysis is both simple and effective.

Scope

The intent of our work has been the development of a simplified method of analysis for use in preliminary design of the penetrator primary structure. Our objectives have been simplicity, rapid turnaround and low cost, in addition to sufficient accuracy for adequate prediction of primary physical processes and associated variables. Our major concerns are stresses and accelerations in the vehicle body itself and stress transmission to the payload shell or liner. (Refer to Figure 1.)

Structural dynamic analysis methods for EPV's presently in use employ large-scale numerical analysis computer codes based upon finite difference or finite element structural models of the vehicle. These codes are very costly and time consuming to use. While these approaches are eminently suited to the final "fine tuning" stage of the vehicle design process, they are ill suited for use in the preliminary design phase where a number of alternative configurations are explored and structural details remain undefined. The present effort, therefore, is not directed toward replacing code calculations but toward supplementing them. We seek a design-oriented method, rather than a capability to analyze fine detail.

At present, our analysis capability is restricted to axisymmetric response of projectiles of revolution due to normal impact events. Existing numerical approaches are similarly limited because three-dimensional

5

analysis of uncoupled loads is not yet possible.

In addition to developing the new approach, it has been applied to the penetrator experiments as mentioned earlier. Reasonable agreement between predictions and measured data at locations on the primary penetrator structure is an important benchmark in validating the new method of analysis.

Basic Approach

The impact and subsequent earth penetration of an EPV is a complex type of phenomenon. A simple description of such a phenomenon is only possible if drastic assumptions can be justifiably made. Several are implicit in our approach; they are essential to achieving our objectives and serve as the groundwork for the new method of analysis.

Considerable effort has been devoted to analyzing the impact and penetration of earth targets under the assumption that the vehicle is rigid. The logic here is that the loads imposed on the vehicle by the target material can be determined in this way as a first step. This is to be followed by an analysis of the vehicle respose to these known loads. This "uncoupling" of the target and vehicle response obviously simplifies the design analysis. It is justifiable if the vehicle stiffness is much greater than that of the target, a condition that is desirable, if not necessary, for successful penetration to great depth. Uncoupled load determination is adopted in our approach.

A second fundamental assumption that underlies the practical utility of our analysis is that the important time period in the vehicle response is just subsequent to impact. We choose, therefore, a stress wave transmission approach to analyze vehicle response. Although in principle

6

a stress wave type of analysis does not restrict our ability to predict long-time response, it does in practice as following reflections from the boundaries of the vehicle becomes quite cumbersome. Furthermore, reflection conditions for portions of the vehicle buried in the target that are consistent with an uncoupled load determination approach are subject to question on physical grounds.

Another important assumption is that the essential nature of the vehicle response is longitudinal and simple bar-like due to normal impact. This implies that one-dimensional plane waves only need be considered and that the stress state is uniaxial. Rotational symmetry of the vehicle about a longitudinal axis and a degree of slenderness of the penetrator are necessary for this assumption to be valid, in addition to a perfectly normal impact/penetration event. A further simplification results if only Hookean elastic material response is considered; this is consistent with the use of very brittle, high strength steels for high velocity penetrator bodies.

The analysis is conducted within the general framework defined by the above assumptions and restrictions. The approach, although general, requires a concrete example, such as that provided by the penetrator experiments conducted by Avco[3], to convey the role of judgment in obtaining good results.

METHOD OF ANALYSIS

Preliminary Remarks

There are three modeling tasks to be completed in order to characterize the impact/penetration event and the EPV. The first is defining the loading environment to which the EPV is exposed; this must be done in a manner that is consistent with the simplicity desired and the one-

7

dimensional bar-like representation of the penetrator primary structure.
An obvious choice is to consider the resultant axial force exerted by
the target as acting at a representative station on the axis of the EPV.

Secondly, as indicated by the sketch in Figure 1, most EPV's can be
viewed as being composed of two distinct portions. There is a forebody
which is highly tapered geometrically*that includes the forward 20 per
cent (approximately) of the total length. The remaining portion of
the vehicle, the aftbody, is rather uniform by comparison. It is natural,
therefore, to model these two regions in different ways appropriate
to their respective physical characteristics. Consequently, idealized
forebody and aftbody models are defined and analyzed separately, as
will be shown in the sequel.

Judgment on the part of the analyst is exercised in defining the
loading, forebody and aftbody models. This is always the situation
if good results are to be obtained by a simple method of analysis.
In the sequel, we present results that are the consequences of our
judgement in describing the penetrator experiments.[3] It is beyond
the scope of our work to consider the sensitivity of predictions to
modeling details.

Loading Idealization

The uncoupled loads on the penetrator for impact into Dakota sand-
stone at 1800 feet per second were calculated.[4] A two-dimensional
finite difference Lagrangian computer code was used. Results are pre-
sented in Reference 4 for pressure distributions at various times, time
histories of pressure at fixed locations and several overall parameters

---

*Some EPV's are tapered over their entire length (all forebody).

8

as functions of time. Figure 6 of Reference 4 is of paramount importance to the present analysis; it shows the calculated resultant axial force time history which serves as the input to our two structural models.

The axial force time history in Figure 6 of Reference 4 contains the typical "noise" or oscillations characteristic of the calculation method. For our purposes, the time history is represented by a series of line segments as shown schematically in Figure 2. The force drops after time t_2 in Figure 2 because the target blocks used in the tests, being of finite extent, have a free outer surface; a relief wave, therefore, is created by a free boundary reflection.

A study of Figure 6 of Reference 4 indicates that our idealized line segment time history model will correspond well if we choose

$$F_o = 43,000 \text{ lbs.} \qquad\qquad t_1 = 160 \text{ microseconds}$$

$$F_1 = 314,000 \text{ lbs.} \qquad\qquad t_2 = 205 \text{ microseconds}$$

$$F_3 = 47,300 \text{ lbs.} \qquad\qquad t_3 = 400 \text{ microseconds}$$

(The above force and time parameters are defined in Figure 2.) It takes a finite time after impact for the axial force to develop appreciable magnitude. Figure 6 of Reference 4 indicates that a 10-microsecond delay in response is appropriate to account for this effect as F_o does not correspond to zero time (impact).

It is also necessary to establish the point of application for the resultant force on the penetrator's longitudinal axis of symmetry. In reality, this "center of force" is time dependent. It moves from the tip of the penetrator nose at the instant of impact to its' aftmost
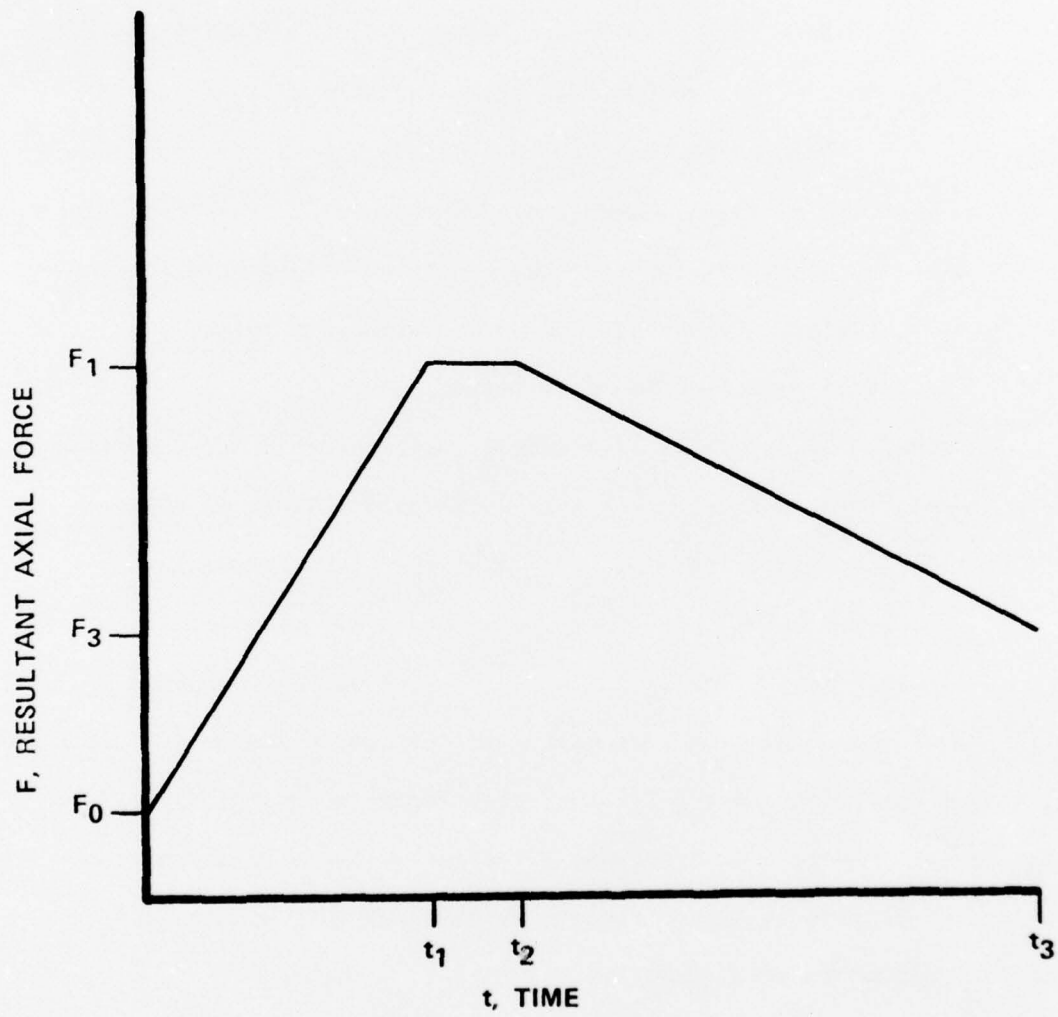
9

Figure 2. Idealized Force Time History

10

location (approximately station 2.05) about 250 microseconds later[4] as the penetrator is progressively encapsulated by the target material. Since accounting for this shift of the center of force with time complicates the analysis beyond the intended scope, a simplification is introduced. The force is assumed to always act at a fixed location. This assumption implies that response variables corresponding to points forward of the aftmost position of the center of force cannot be estimated on a rational basis. In view of this, the aftmost location, station 2.05, is selected as the fixed location.

The above approach, although there is no uniqueness associated with our choice for the effective center of force, is the simplest way to treat the progressive encapsulation by the target material. Any other approach involves time-wise numerical solution of equations, which is certainly to be avoided if the original objectives are to be met. Detailed information on the nose tip region is sacrificed in order to obtain the great simplicity demonstrated in the following sections.

Forebody Model and Analysis

The forebody portion of the EPV is characterized by a high degree of geometric taper. Ogive shapes are the usual choice. A sketch of our forebody model is shown in Figure 3. The origin for the longitudinal coordinate x (positive aftward) is taken at the assumed center of force. Note that the nose portion forward of this point is not loaded according to this idealized model; it contributes, therefore, only a mass M which acts effectively at the origin. Uniaxial, simple bar-like response is characterized by the single longitudinal displacement
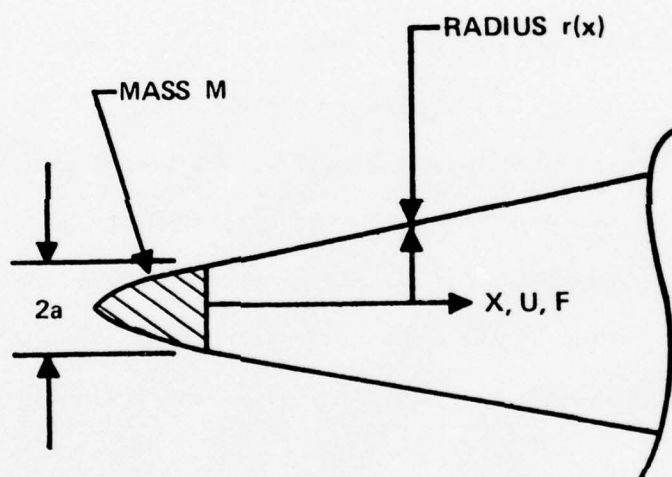
11

Figure 3. Forebody Model

$u(x,t)$ which describes the translation of the cross section at x for
any time t.

The differential equation governing longitudinal motion of a homo-
geneous bar with varying cross sectional area A is

$$(EAu,_x),_x - \rho Au,_{tt} = 0 \tag{1}$$

The elastic modulus is E and ρ is the mass density of the bar material.
This equation is valid provided that the bar is slender and the variation
of A is smooth and not too severe; if these conditions are not met,
three-dimensional effects become important, thereby tending to undermine
the accuracy of this simple theory.

A further simplification results if we restrict out attention to
tapered bars of revolution with a linearly varying outer radius; in
this case, an exact solution has been found to Equation (1). This
"conical" approximation describes the major, first order influence of
geometric taper. The radius $r(x)$, then, satisfies an equation of the
form

$$r(x) = a + \alpha x \tag{2}$$

The radius at the origin is a, and α is a parameter characterizing
the taper. The cross sectional area is

$$A(x) = \pi (a + \alpha x)^2 \tag{3}$$

Equation (1) can be written in the following form:

$$u,_{xx} + \frac{2\alpha}{(a + \alpha x)} u,_x - \frac{1}{c^2} u,_{tt} = 0 \tag{4}$$

13

The velocity of propagation of disturbances in the bar is $c = \sqrt{E/\rho}$.

The solution to Equation (4) for a wave traveling in the positive x-direction is

$$u(x,t) = \frac{a}{(a + \alpha x)} \; f(t - \frac{x}{c}) \tag{5}$$

f is an arbitrary function to be determined by the boundary condition at x = 0. The validity of this solution is easily verified by direct substitution into Equation (4).

The appropriate boundary condition to be applied to x = 0 corresponds to the equation of motion for the mass M. It may be written as follows

$$M \, u_{,tt}(0,t) = F(t) + EA(0) \, u_{,x}(0,t) \tag{6}$$

With the aid of Equations (3) and (5), this result may be simplified to

$$Mf''(t) + \frac{\pi a^2 E}{c} f'(t) + \pi a \, \alpha E f(t) = F(t) \tag{7}$$

The notation ( )' is used to indicate an ordinary derivative with respect to the argument of the function. The mass M is small compared to the total mass of the model. Consequently, a simplification results if the M-term is neglected in (7). The following simplified equation results:

$$f'(t) + \frac{\alpha c}{a} \; f(t) = \frac{c}{\pi a^2 E} \; F(t) \tag{8}$$

14

This equation reflects the effect of taper by the presence of the parameter α .

The solution to Equation (8) can be written for arbitrary $F(t)$ with the aid of the indicial admittance function $\bar{A}(t)$. $\bar{A}(t)$ is defined as the solution corresponding to a unit step function force distribution; it is *

$$\bar{A}(t) = \frac{1}{\pi a \alpha E} (1 - e^{-\frac{\alpha c}{a} t}) \qquad (9)$$

The general solution for arbitrary $F(t)$ is

$$f(t) = \int_0^t F(\tau) \, \bar{A}'(t-\tau) \, d\tau \qquad (10)$$

For early times $(t \leq t_1)$, the force distribution according to our loading model shown in Figure 2 can be written as

$$F(t) = F_0 + \frac{(F_1 - F_0)}{t_1} t \qquad (t \leq t_1) \qquad (11)$$

For this distribution

$$f(t) = \frac{F_0}{\pi a \alpha E} (1 - e^{-\frac{\alpha c}{a} t}) \qquad (12)$$

$$+ \frac{(F_1 - F_0)}{t_1 \pi \alpha^2 c E} \left[\frac{\alpha c}{a} t - 1 + e^{-\frac{\alpha c}{a} t} \right] \qquad (12)$$

The axial strain $\epsilon_x(x,t)$ can be determined from $f(t - \frac{x}{c})$ and Equation (5). The result can be written as follows:

---

*The initial condition $\bar{A}(0) = 0$ has been used to obtain this result.

15

$$\epsilon_x(x,t) = u_{,x} = C_1 e^{-\frac{\alpha c}{a}\left(t - \frac{x}{c}\right)} + C_2 + C_3\left(t - \frac{x}{c}\right) \tag{13}$$

The functions C_1, C_2 and C_3 are

$$C_1 = \frac{F_0}{\pi E(a + \alpha x)}\left[\left(\frac{1}{a} - \frac{1}{(a+\alpha x)}\right)\right]$$
$$+ \frac{(F_1 - F_0)}{t_1 \pi E \alpha c}\left[\frac{a}{(a+\alpha x)^2} - \frac{1}{(a+\alpha x)}\right] \tag{14}$$

$$C_2 = \frac{F_0}{\pi E(a+\alpha x)^2} + \frac{(F_1 - F_0)}{t_1 \pi E \alpha c}\left[\frac{1}{(a+\alpha x)} - \frac{a}{(a+\alpha x)^2}\right] \tag{15}$$

$$C_3 = \frac{(F_1 - F_0)}{t_1 \pi E(a+\alpha x)^2} \tag{16}$$

In applying the above results to the penetrator shown in Figure 1, the fact that the nose region is composed of two materials has been ignored. The properties of the steel outer shell have been used. The appropriate parameter values are

$$\alpha = 0.2126$$
$$c = 197,174 \text{ inches/sec}$$
$$a = 0.874 \text{ inches}$$
$$E = 28.5 \times 10^6 \text{ psi}$$

It will be apparent from the discussion of results that this approximation for the forebody provides excellent strain predictions.

Aftbody Model and Analysis

In contrast to the EPV forebody, the primary load carrying structure
of the aftbody is relatively uniform in geometry and stiffness. As
a first approximation, therefore, the analytical model is based upon
uniform or nominal stiffness for the entire length of the aftbody.
The forebody's influence is confined to introducing a (usually substan-
tial) mass M_0 in the most forward location and a path for transmitting
the resultant force F. This idealized model is shown in Figure 4.
There are two uniform elastic bars which act in parallel connected to
M_0. This is because the outer body shell and inner liner or payload
shell of the penetrator shown in Figure 1 are separated by an air gap
and do act as independent load transmission paths.

We use the subscript "1" for the bar corresponding to the outer
body shell and "2" for the payload shell. The structural effect of
the potting material used in the payload module (Figure 1) is neglected
completely. Since the bars are assumed to be uniform, traveling waves
in the positive x-direction in the bars are represented by the functions
$g_1(t - \frac{x}{c_1})$ and $g_2(t - \frac{x}{c_2})$. Physically both bars are attached to the
mass M_o at the origin; therefore

$$g_1(t) = g_2(t) \equiv g(t) \tag{17}$$

A boundary condition, similar to Equation (6) and expressing the
equation of motion for M_o, can be formulated for use in determining
g. It is

$$M_o \, g''(t) + \left(\frac{E_1 A_1}{c_1} + \frac{E_2 A_2}{c_2} \right) g'(t) = F(t) \tag{18}$$
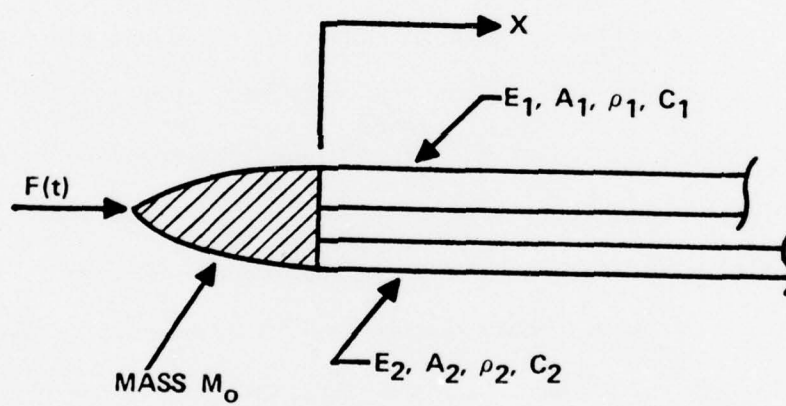
17

Figure 4. Aftbody Model

Also, we require

$$g(0) = g'(0) = 0 \qquad (19)$$

as the bars are at rest initially.

It is convenient to introduce the parameter μ defined as

$$\mu = \frac{1}{M_o} \left(\frac{E_1 A_1}{c_1} + \frac{E_2 A_2}{c_2} \right) \qquad (20)$$

Equation (18), then, is equivalent to

$$g'' + \mu g' = \frac{F(t)}{M_0} \qquad (21)$$

By analogy with the solution process used to determine f for the fore-body model, we seek the response due to a unit step function force. Let $\bar{v}$ be the velocity (g') for a unit step force input; it is given by the following expression:

$$\bar{v} = \frac{1}{M_0} (1 - e^{-\mu t}) \qquad (22)$$

The velocity corresponding to an arbitrary force F(t) is, therefore

$$v \equiv g' = \int_0^t F(\tau)\, \bar{v}'(t - \tau)\, d\tau = \frac{1}{M_0} \int_0^t e^{-\mu(t - \tau)} F(\tau)\, d\tau \qquad (23)$$

The force time history model defined in Figure 2 is characterized by three distinct analytical expressions, one corresponding to each line segment. They are

19

$$F(t) = F_0 + \frac{(F_1 - F_0)}{t_1} t \qquad (0 \leq t \leq t_1) \qquad (11)$$

$$F(t) = F_1 \qquad (t_1 \leq t \leq t_2) \qquad (24)$$

$$F(t) = F_1 - \frac{(F_1 - F_3)}{(t_3 - t_2)} (t - t_2) \qquad (t_2 \leq t \leq t_3) \qquad (25)$$

These expressions may be substituted into (23) to determine the particle velocity v. The axial strains, then, in bars 1 and 2 are found from the following equations:

$$\epsilon_{x1} = g_{1,x} = -\frac{1}{c_2} v(t - \frac{x}{c_1}) \qquad (26)$$

$$\epsilon_{x2} = g_{2,x} = -\frac{1}{c_2} v(t - \frac{x}{c_2}) \qquad (27)$$

These theoretical results have been applied to the aftbody (the portion of the penetrator aft of station 8) of the penetrator shown in Figure 1. The following parameter values have been used in the analysis:

$E_1 = 28.5 \times 10^6$ psi $\qquad\qquad E_2 = 26.5 \times 10^6$ psi

$c_1 = 197,174$ in/sec $\qquad\qquad c_2 = 188,141$ in/sec

$A_1 = 3.0$ in^2 $\qquad\qquad A_2 = 0.4$ in^2

$M_0 = 0.0415 \frac{\text{lb.-sec}^2}{\text{in}}$ $\qquad\qquad \mu = 11,871$ sec^{-1}

The results for a semi-infinite aftbody are*

_____

*The units of velocity used are inches per second.

20

$$v = 87.4 \ (1 - e^{-\mu t}) + 289.7 \left[\mu t - (1 - e^{-\mu t}) \right] \ (0 \le t \le t_1) \quad (28)$$

$$v = e^{-\mu t} \left[2533.9 + 638.1 \ (e^{\mu t} - 6.7) \right] \quad (t_1 \le t \le t_2) \quad (29)$$

$$v = 5541.0 \ e^{-\mu t} + 638.1 \ (1 - e^{-\mu(t - t_2)} - 25.9 \left[(\mu t - 1) - 1.4 \ e^{-\mu(t - t_2)} \right]$$

$$(t_2 \le t \le t_3) \quad (30)$$

A graphical representation of the strain in bar 1 obtained using Equations (28) - (30) appears in Figure 5.

As is usual in wave transmission analyses of the present kind, baseline information is provided by the semi-infinite model solution described above and shown in Figure 5. The effect of finite penetrator length is accounted for by appropriate reflection conditions at the aft end. Superposition of traveling wave solutions is used to satisfy the aft end boundary condition, thereby providing an exact solution for dynamic response consistent with the loading and penetrator models. A convenient method of treating reflections is described in the Appendix.

Synopsis of the Method

Our method of analysis is summarized briefly as follows:

(1) Define loading, forebody and aftbody models;

(2) Determine the response of the forebody and aftbody models as if they are semi-infinite in length;

(3) Use superposition of the semi-infinite traveling wave solutions to satisfy appropriate boundary conditions that correspond to finite penetrator length.

Corresponding to any model definitions, the response is obtained from simple closed form expressions and their superposition. As will be
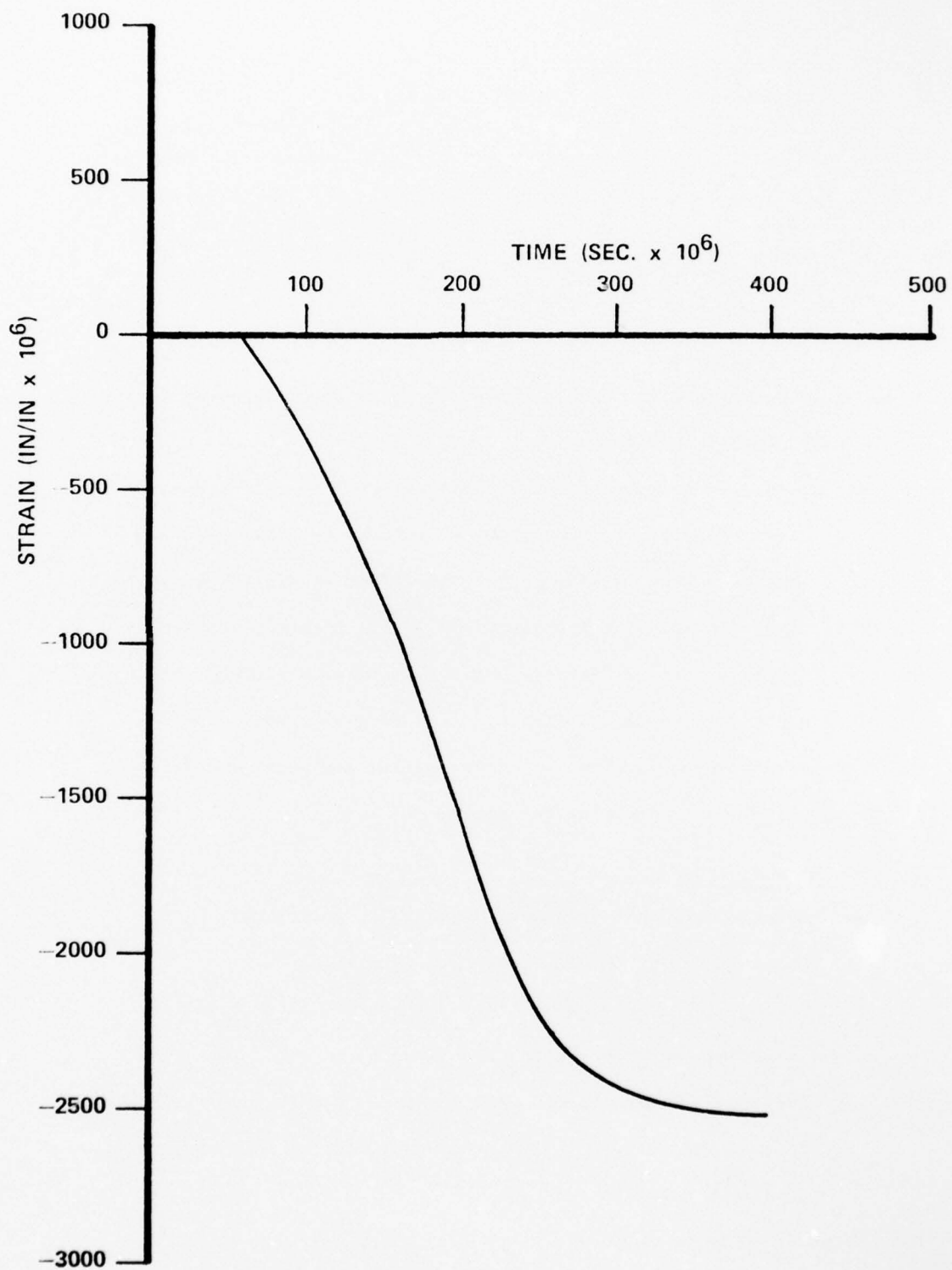
Figure 5.   Response of Bar 1 for a Semi-Infinite Aftbody Model

shown next, this simplicity is also accompanied by excellent agreement
with available experimental data on response of the primary structure.

RESULTS AND DISCUSSION

Preliminary Remarks

From the outset, our primary concern has been predicting the response
of the load carrying structural elements by simple means. Simplicity
and ease of application have certainly been achieved. We now show that
our approach also provides excellent quantitative predictions for strains
and accelerations.

In the following, strain and acceleration predictions are discussed
separately, as are the response of the penetrator main body outer shell
and the internal structure. This way of categorizing the results is
both convenient and useful in judging the validity of the modeling
assumptions.

The analytical results presented are directly comparable to the
experimental ones that are given in Reference 3. While our intent is
not to provide an exhaustive correlation study, representative experi-
mental data are presented on the same figures with theoretical predictions
in several instances. These selected benchmarks are sufficient to
illustrate the generally fine degree of agreement between theory and
experiment that has been achieved.

Outer Shell Strain Predictions

Axial strains have been measured at four locations on the exterior
of the penetrator main body outer shells during the two tests.[3] Station 4,

the most forward location, is the only site on the penetrator forebody.
The remaining sites are stations 9, 19.5 and 27.3 on the aftbody.
Theoretical axial strain time histories determined by our analysis
method for these locations appear in Figures 6-9.

The strain gages at station 4 are wiped off during the penetration
of the target. Consequently, only short-time data is available. In
this case, only the force representation in Equation (11) need be con
sidered. From a study of Figure 1, it is to be expected that reflections
of the primary stress wave will be produced at station 8 where the uranium
ballast plug ends. Station 8 behaves approximately as a free end for
the forebody, while the buried portion of the penetrator nose can be
considered fixed. As a consequence of these double reflections, the
experimental data in Figure 6 exhibits two noticeable pauses in the
otherwise monotonic trend. The theoretical prediction is for a semi-
infinite forebody, so the pauses do not occur in that curve. Clearly,
there is excellent agreement otherwise, and it is apparent that the
first passage semi-infinite prediction is a conservative design esti-
mate.

Response at station 4 has been studied extensively. The theoret-
ical results presented in Figure 6 account for the mass M (Equation
(7)). Another solution based upon Equations (8) and (13) is in close
agreement. Attempts to account for the double reflection pauses have
met with reasonable success also. For brevity, only the one prediction
is shown.

The strain predictions at stations 9, 19.5 and 27.3 in Figures
7-9 have all been obtained from the semi-infinite aftbody model response
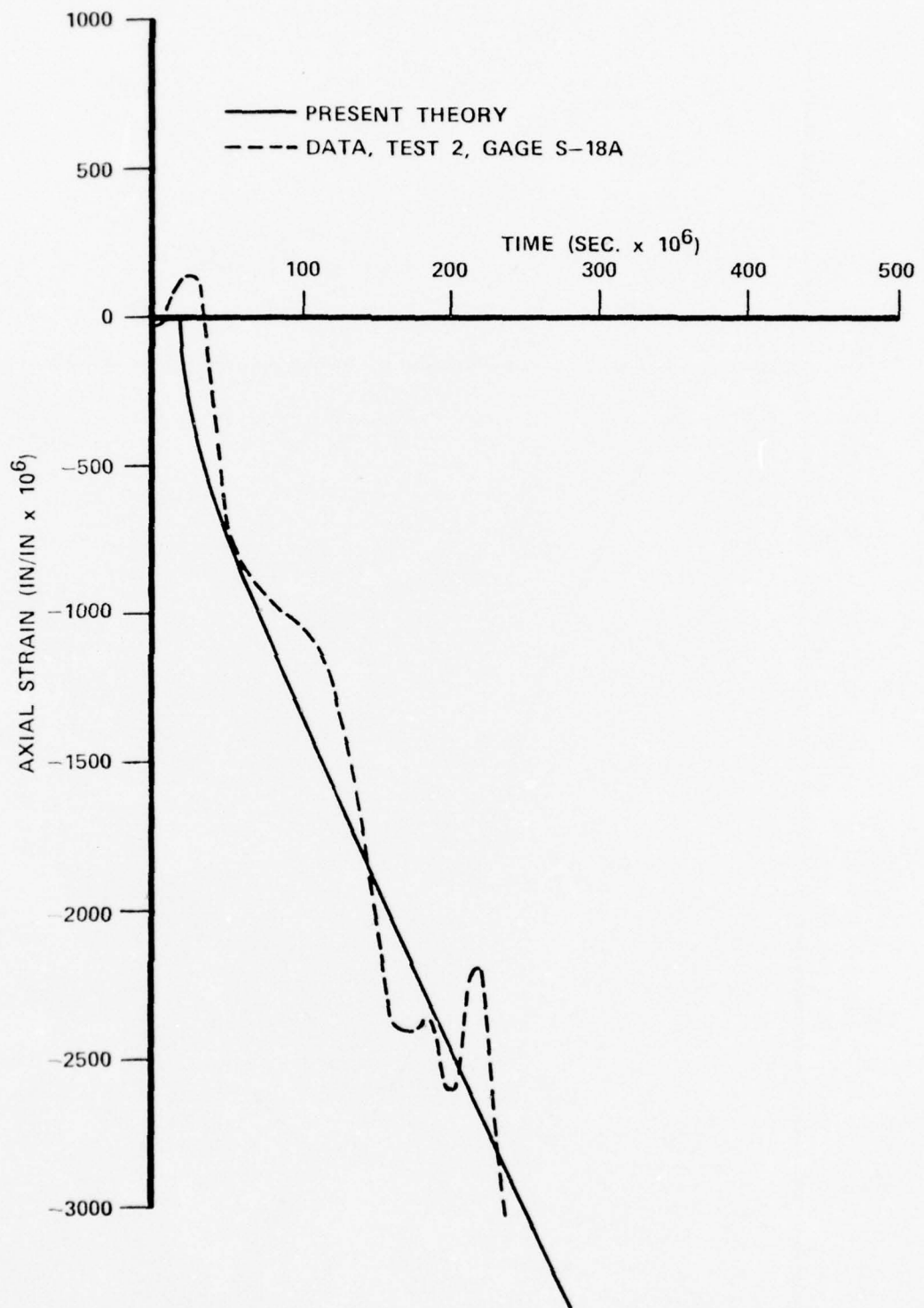
24

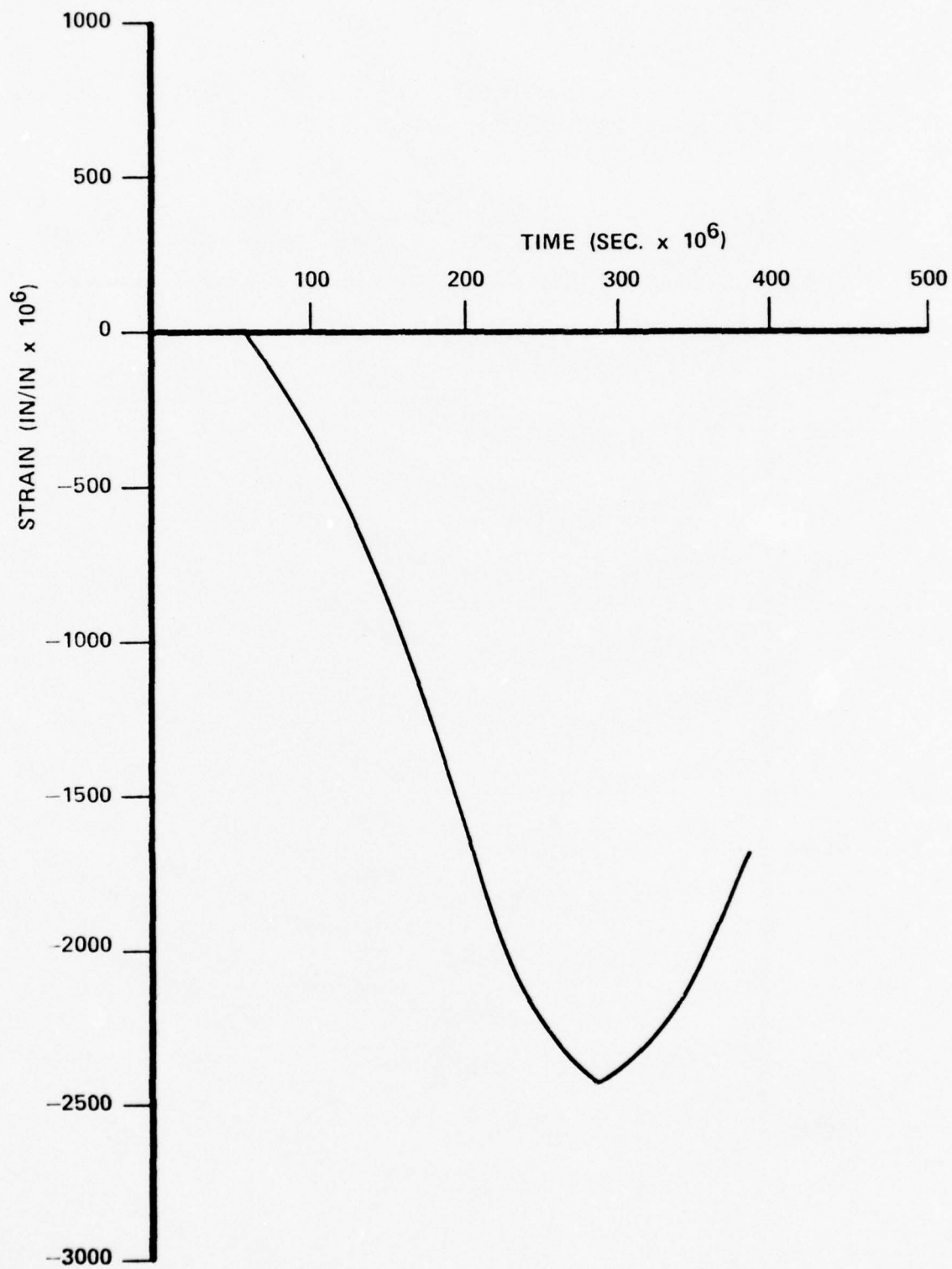Figure 6.   Axial strain at Station 4 - Outer Shell

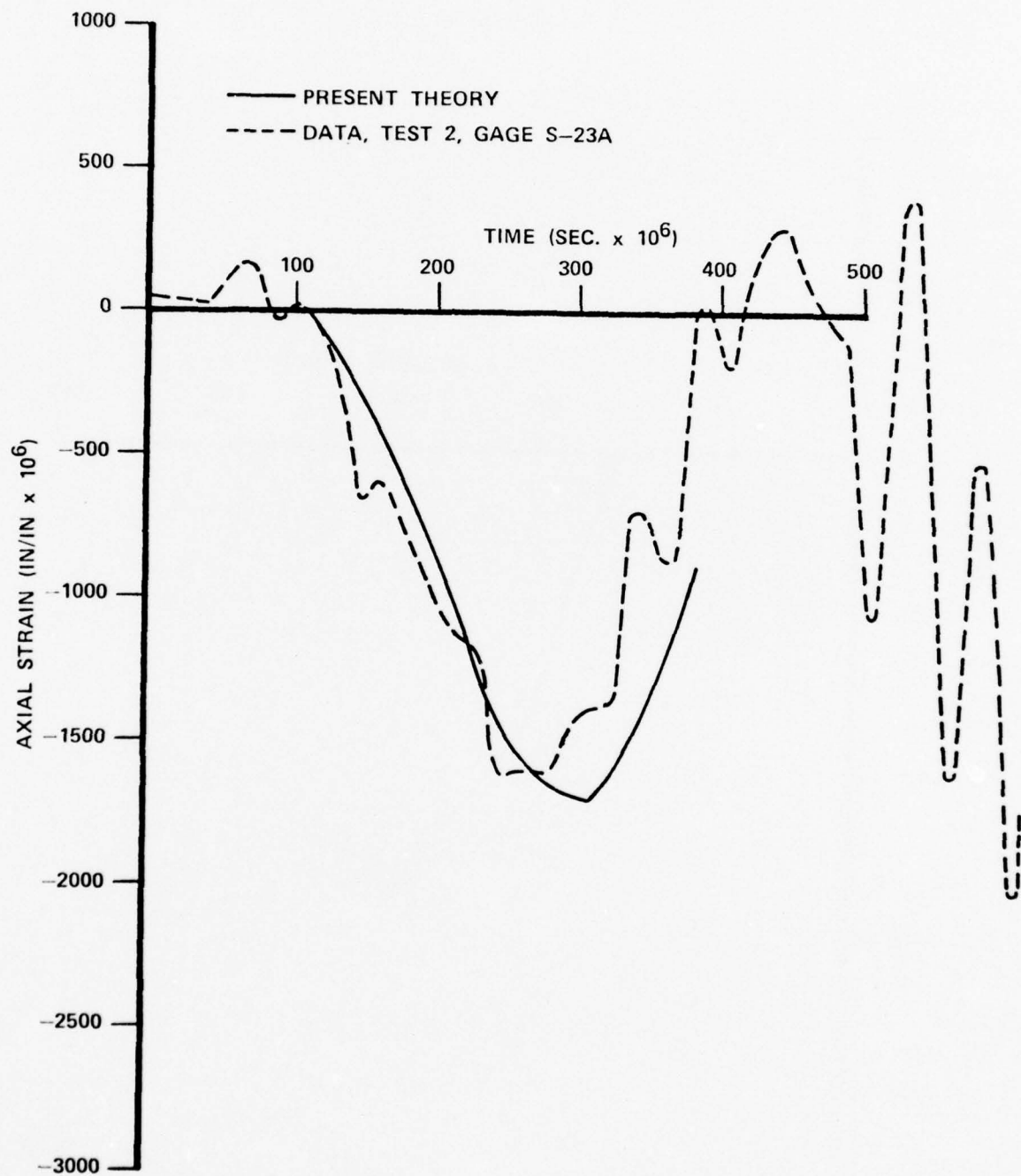Figure 7. Axial Strain at Station 9 - Outer Shell

26

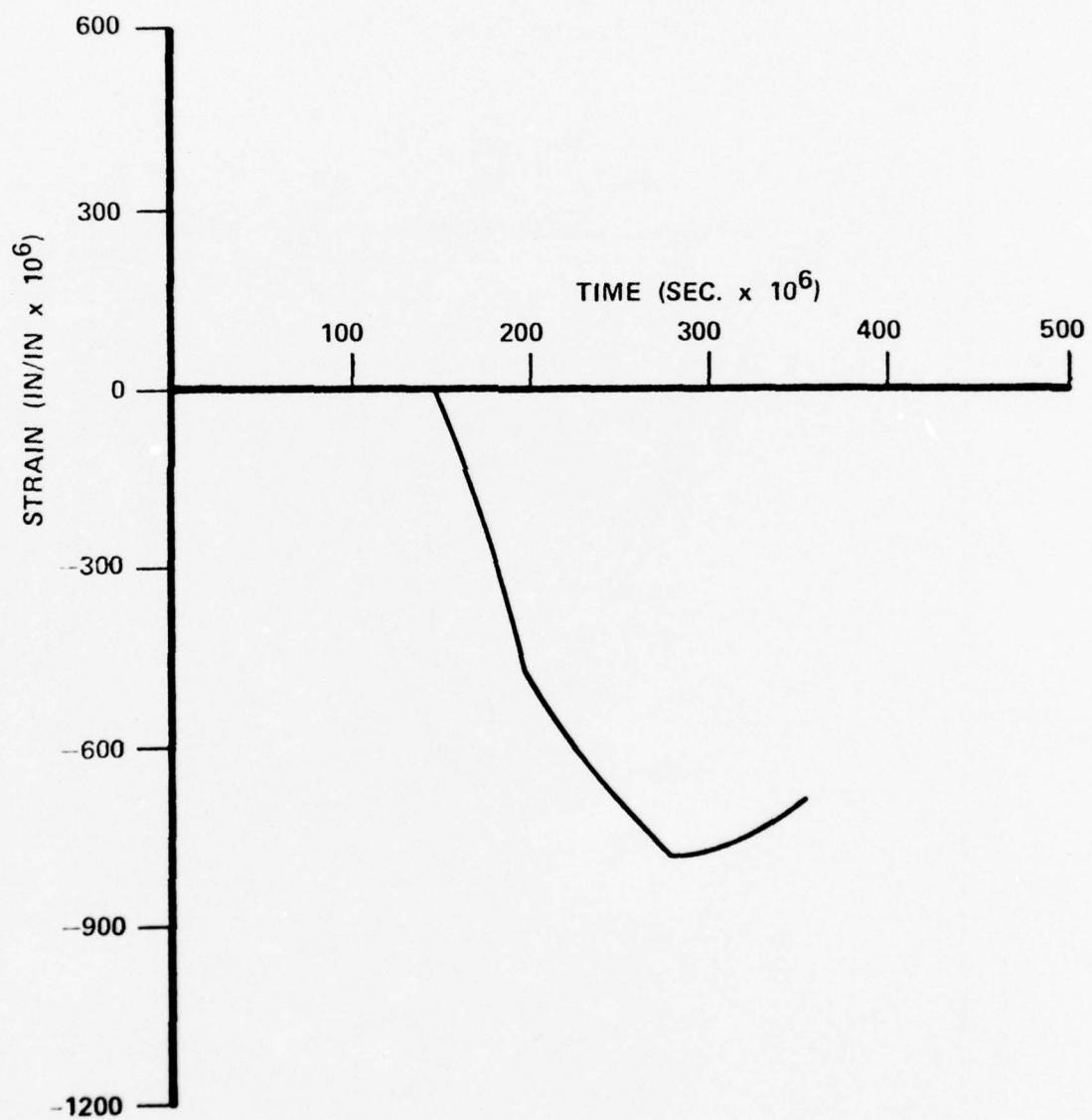Figure 8. Axial Strain at Station 19.5 - Outer Shell

Figure 9. Axial Strain at Station 27.3 - Outer Shell

28

shown in Figure 5. The aft end of the outer shell at station 32 behaves essentially as a free end. Consequently, a relief wave is generated which is opposite in sign (tensile) to the incident (compressive) wave; a simple graphical approach to superimposing the effects of these two waves is given in the Appendix. The arrival of the relief wave at each station is easily identified in the figures.

The prediction for station 19.5 is compared with experimental data in Figure 8. Note that a shift to the left of 25 microseconds in the theoretical curve would produce nearly perfect agreement between theory and experiment. The time scale of the experimental data is only accurate to within this time increment.[3] Although no effort has been made to adjust the time origin for improved agreement, this particular case is conspicuous in that a shift produces striking agreement.

Strain Predictions For Internal Structure

The payload shell or liner is the primary load carrying element in the interior of the penetrator. The shell is not continuous, but segmented in a modular fashion. The segments are threaded at the ends with the joints reinforced by rings.[1] It is to be expected, therefore, that variability in these mechanical joints makes the precise nature of the load transmission path indeterminant in practice.

Our aftbody model is based upon continuity of the payload shell; the joints and small reinforcing rings are totally ignored. There are two very large titanium rings[1] located at stations 23.25 and 31.25 (Figure 1) which cannot be ignored, however.

The two titanium rings have been modeled as concentrated masses attached to the payload shell. The addition of a concentrated mass

29

to an elastic bar is analyzed in detail in Reference 5. Initially,
the concentrated mass produces a reflection of the incident stress wave
as if the mass is a fixed end; the reflection decays exponentially with
time thereafter. Simultaneously, the stress wave transmitted beyond
the mass builds up exponentially until the original incident stress
level is reached. For stations forward of the first ring, it is con-
servative to assume that a fixed end reflection occurs.

Axial strain data has been obtained at two stations on the inside
of the payload shell, stations 9 and 19.5, forward of the first titanium
ring. The theoretical predictions shown in Figures 10 and 11 are based
upon the assumption of a fixed end at the first ring. The station 9
prediction, although slightly conservative, agrees very well with the
experimental data from Reference 3. In Figure 11, representative ex-
perimental data is also presented for station 19.5; note that the pre-
diction indicates a more rapid strain build-up than the measured data
(a conservative trend), although the peak strain values are in good
agreement.

Axial strain has been measured also at station 31.5 on the inside
of the payload shell. This location is aft of both large titanium
rings. The measured strain is much smaller in magnitude than the others
and opposite in sign (tensile)[3]. Our modeling approach to these rings
would suggest that the strain at this location is essentially zero in
the time period of interest; consequently, there is no predicted time
history included.

In addition to the payload shell, strain gages were mounted on
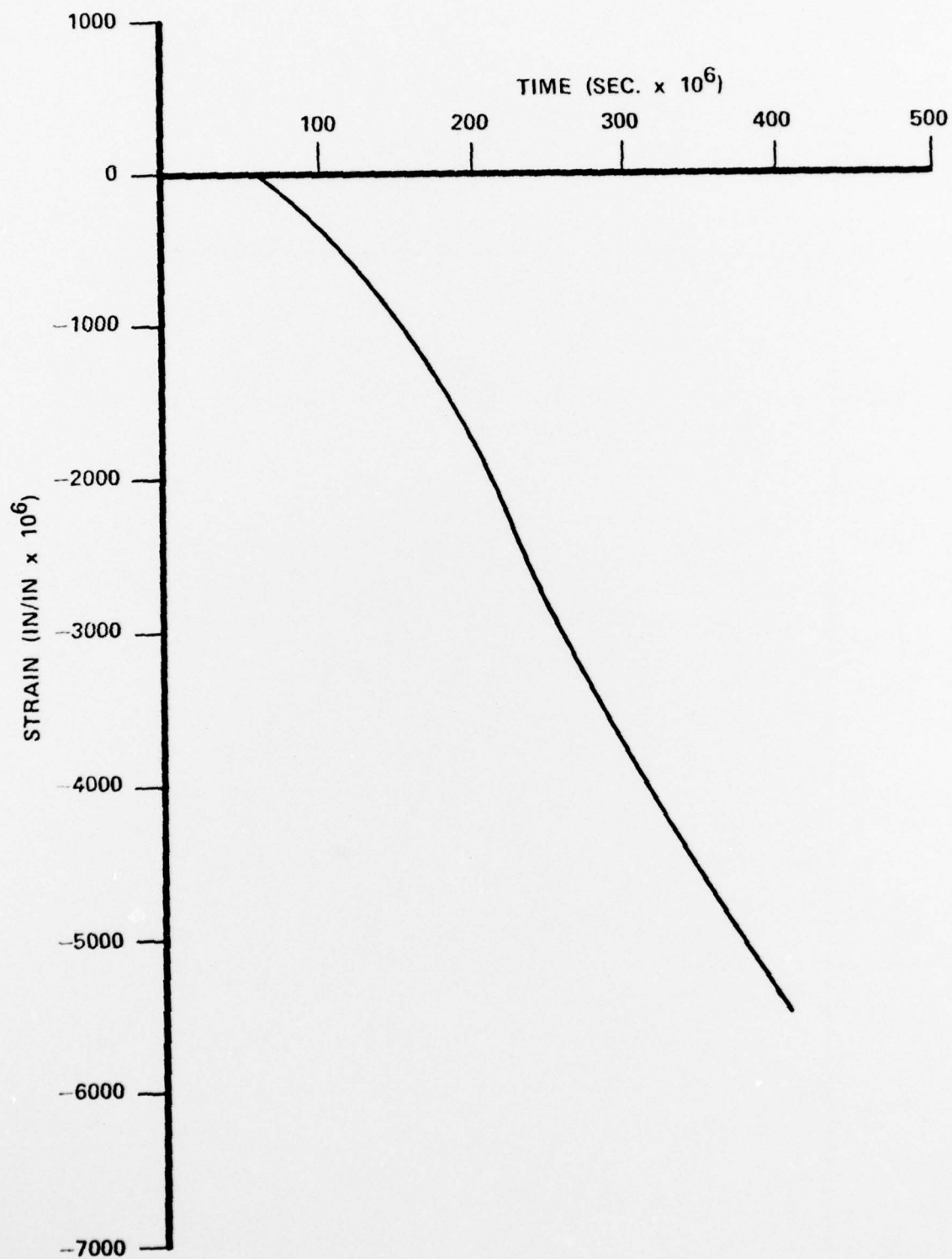the flexible potting material at Station 16. Our aftbody model does

30

Figure 10. Axial Strain at Station 9 - Inner Payload Shell
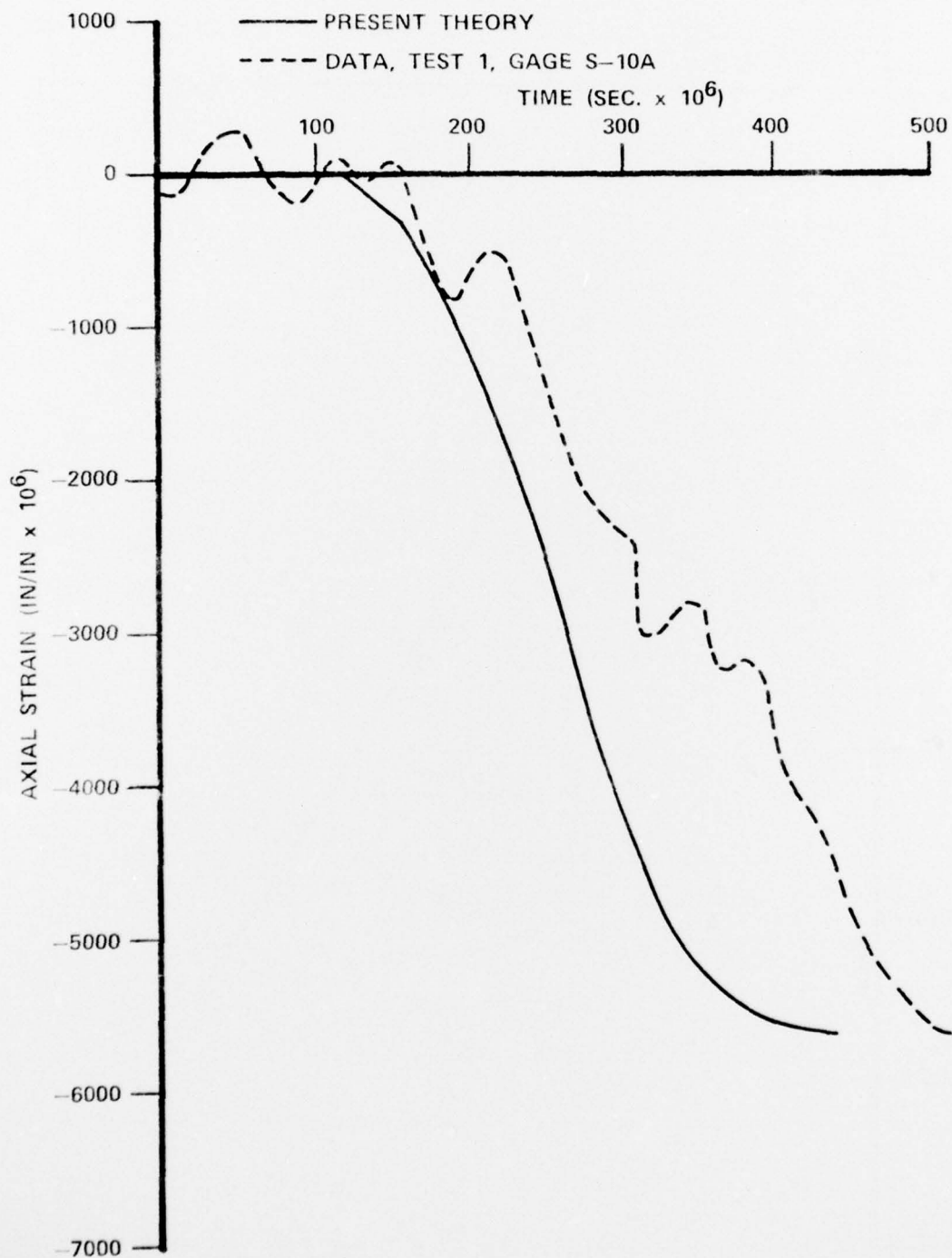
31

Figure 11. Axial Strain at Station 19.5 Inner Payload Shell

32

not account for any contribution by the potting to structural stiffness as it is quite small. The axial strain in the potting can be estimated, however, if strain compatibility with the payload shell is assumed. This approximation results in a potting axial strain at Station 16 that is essentially identical to that in the payload shell at station 19.5 with a slight shift of the time axis; the same prediction curve suffices, therefore. This is in good agreement with the experimental results given in Reference 3.

Hoop Strain Predictions

All hoop strains correspond to simple Poisson expansion only according to our simple bar-like models. Consequently, separate results for the hoop strains are not presented. This simple uniaxial stress state is a good approximation over most of the penetrator.[3] It cannot be applied at Station 4, however, where three-dimensional effects due to nose encapsulation obviously occur; prediction of these effects is beyond the scope of our approach.

Acceleration Predictions

Two accelerometers were mounted on primary load carrying structure for the Avco tests, one forward at Station 7 and one aft at station 32[1]. Acceleration predictions for these locations are presented in Figures 12 and 13, respectively . These predictions have been determined using the aftbody model.

Also shown in Figure 13 is data from Reference 3 for comparison. The trends correspond quite well, but a high frequency oscillation in the test data is not predicted by our analysis.
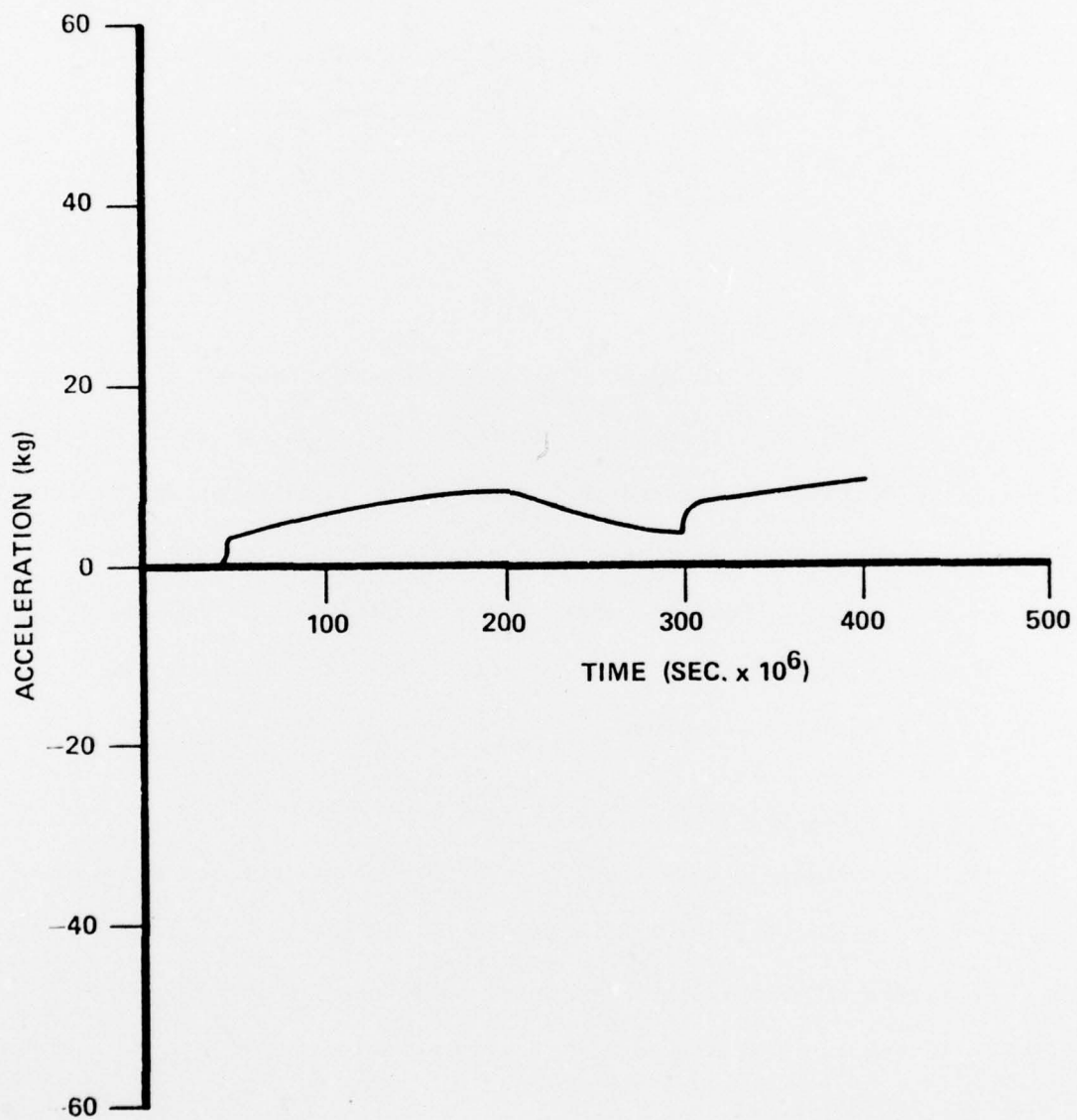
33
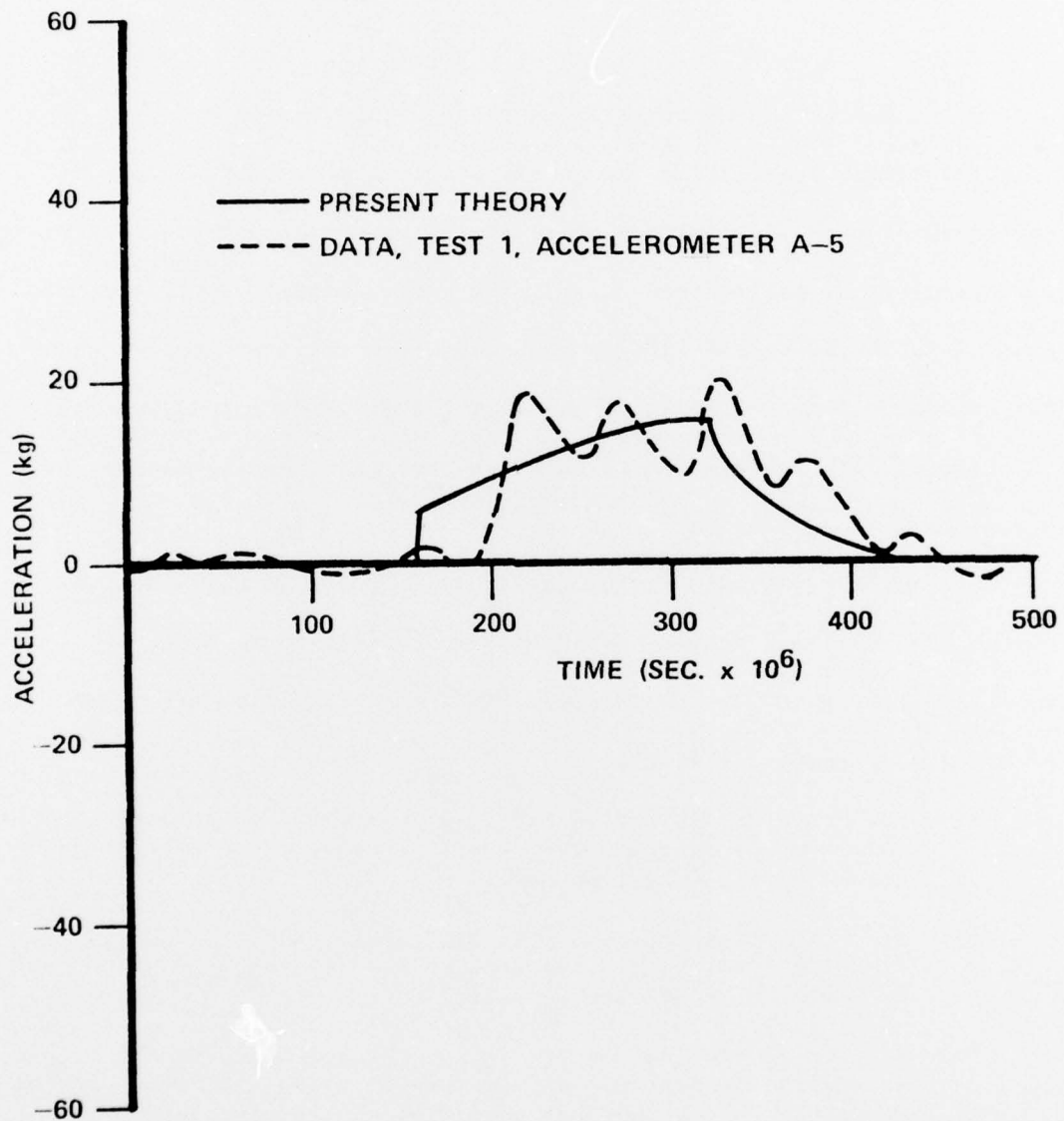
Figure 12. Axial Acceleration at Station 7

34

Figure 13. Axial Acceleration at Station 32

35

CONCLUSIONS AND RECOMMENDATIONS

The work presented here is a pioneering effort to develop a simple, reliable preliminary design analysis method for normal impact of earth penetrators. In addition, the method has been applied to predict the outcome of actual impact/penetration tests. The results obtained for this particular application are in excellent agreement with available experimental data associated with locations on the primary load carrying structure of the penetrators tested. We conclude, therefore, that the objectives stated in the introduction have been met. We believe that the approach is basically sound and that the evidence supporting this conclusion, although limited to only one penetrator configuration, is never-the-less convincing.

The method, although useful as far as it goes, is still not yet beyond the embryonic stage. Additional work needs to be done, and several questions remain unanswered. The following items are examples of areas that require attention:

(1) Explore alternatives to the fixed center of force approach which better describe the dynamic encapsulation of the penetrator by the target material;

(2) Study the limitations on the applicability of the one-dimensional models; (e.g., how slender must the penetrator be for the bar-like models to be valid?)

(3) Develop simple loading prediction methods which do not require large-scale numerical calculations or which are not empirical in nature. These methods should be in the same spirit as the present penetrator response analysis;

(4) Verify the validity of the method for penetrators which differ substantially in configuration from the ones considered here;

(5) Refine the forebody model to account for second order effects of taper;

(6) Develop similar models and an analysis method that applies to non-normal impact events;

(7) Develop solutions valid for long-time response and match them to the short-term wave analysis.

The above listing order does not imply an order of priority. Successful accomplishment of these tasks will insure that the desired design analysis capability will be effective and accepted by penetrator analysts and designers.

REFERENCES

1. McCoy, D., and Sieradzki, F., "DNA Reverse Ballistic EP Proposal", Drawing Number S17186, Sandia Corporation.

2. Hadala, P. F., Letter on Location of Accelerometers and Strain Gages on One-Half Scale Earth Penetrators, January 5, 1976 (with enclosed diagram).

3. Avco Corporation, "DNA Reverse Ballistic Test Data Package", supplied to DNA contractors in October 1976.

4. Wagner, M. H., Fulton C. C., and Goerke, W. S., "Calculation of Reverse Ballistic Test into Dakota Sandstone at 1800 Feet/Second", California Research and Technology, Inc., Woodland Hills, California, report for contract DNA 001-76-C-0157, February 1976.

5. Timoshenko, S. P., and Goodier, J. N., Theory of Elasticity, Third Edition, McGraw-Hill, 1970, pp. 498-504.

APPENDIX

A Simple Graphical Approach for Wave Reflection Analysis

As indicated in the discussion of the aftbody model, baseline
information for a wave transmission analysis is provided by a semi-
infinite model solution as shown in Figure 5. The effect of finite
penetrator length is accounted for by appropriate reflection conditions.
For clarity, we will outline the approach used to satisfy free end
conditions at the aft end of the main body outer shell.

At a free end, the axial stress, and hence the axial strain, is
zero for all time. This condition is satisfied if a wave of opposite
sign but same geometric form as the incident wave travels in the opposite
direction in the bar; the incident semi-infinite model wave and the
"reflected" wave of opposite sign must be timed such that the sum of
the axial strains due to both waves is always zero at the end point.
The strain distribution within the penetrator at any time prior to the
time that the reflected wave reaches the forward end is the sum of the
contributions due to the two waves.

This superposition is easily accomplished graphically as follows.
For a given location on the penetrator, the arrival times for the in-
cident semi-infinite solution strain wave and the free end reflected
wave of opposite sign are determined for the wave speed of the material.
Between these two times, the solution is the same form as the semi-
infinite solution with origin at the former time. For times after the
latter arrival time, appropriate increments must be subtracted from

the incident wave strain values to correspond to a reflected wave moving in the opposite direction; the origin of the reflected wave is the latter arrival time. This superposition is easily accomplished with the aid of a light table, copies of the semi-infinite incident wave profile, and dividers. The resulting profile for a particular station can be determined quite rapidly in this way.

Fixed end conditions require addition of like strain wave profiles, rather than subtraction. Acceleration profiles may be obtained in a similar manner, but the role of addition and subtraction are exactly reversed for accelerations due to free and fixed ends.

DISTRIBUTION LIST

DEPARTMENT OF DEFENSE

Director
Defense Advanced Research Proj. Agency
    ATTN: Technical Library

Director
Defense Civil Preparedness Agency
Assistant Director for Research
    ATTN: Admin. Officer

Defense Documentation Center
Cameron Station
12 cy ATTN: TC

Director
Defense Intelligence Agency
    ATTN: DT-2, Wpns. & Sys. Div.
    ATTN: Technical Library
    ATTN: DI-7E
    ATTN: Charles A. Fowler
    ATTN: DB-4C, Edward O'Farrell

Director
Defense Nuclear Agency
    ATTN: DDST
    ATTN: SPAS
5 cy ATTN: SPSS
    ATTN: TISI, Archives
3 cy ATTN: TITL, Tech. Library

Dir. of Defense Research & Engineering
Department of Defense
    ATTN: S&SS (OS)

Commander
Field Command
Defense Nuclear Agency
    ATTN: FCPR

Director
Interservice Nuclear Weapons School
    ATTN: Document Control

Director
Joint Strat. Target Planning Staff, JCS
    ATTN: STINFO, Library

Chief
Livermore Division, Field Command, DNA
Lawrence Livermore Laboratory
    ATTN: FCPRL

DEPARTMENT OF THE ARMY

Dep. Chief of Staff for Research Dev. & Acq.
Department of the Army
    ATTN: DAMA(CS), Major A. Gleim
    ATTN: Technical Library
    ATTN: DAMA-CSM-N, LTC G. Ogden

Chief of Engineers
Department of the Army
2 cy ATTN: DAEN-RDM
2 cy ATTN: DAEN-MCE-D

DEPARTMENT OF THE ARMY (Continued)

Deputy Chief of Staff for Ops. & Plans
Department of the Army
    ATTN: Dir. of Chem. & Nuc. Ops.
    ATTN: Technical Library

Chief
Engineer Strategic Studies Group
    ATTN: DAEN-FES

Commander
Frankford Arsenal
    ATTN: L. Baldini

Project Manager
Gator Mine Program
    ATTN: E. J. Linddsey

Commander
Harry Diamond Laboratories
    ATTN: DRXDO-RBH, James H. Gwaltney
    ATTN: DRXDO-NP

Commander
Picatinny Arsenal
    ATTN: SMUPA-AD-D-A-7
    ATTN: Marty Margolin
    ATTN: SMUPA-AD-D-M
    ATTN: SMUPA-AD-D-A
    ATTN: DR-DAR-L-C-FA, B. Shulman
    ATTN: P. Angelloti
    ATTN: Ray Moesner
    ATTN: Technical Library
    ATTN: Paul Harris
    ATTN: Jerry Pental
    ATTN: Ernie Zimpo

Commander
Redstone Scientific Information Center
US Army Missile Command
    ATTN: Chief, Documents

Commander
US Army Armament Command
    ATTN: Tech. Lib.

Director
US Army Ballistic Research Labs.
    ATTN: DRXBR-TB
    ATTN: DRXBR-X
    ATTN: DRDAR-BLE, J. H. Keefer
    ATTN: G. Roecker
    ATTN: A. Ricchiazzi
2 cy ATTN: Tech. Lib., Edward Baicy
    ATTN: G. Grabarek
    ATTN: J. W. Apgar

Commander & Director
US Army Cold Region Res. Engr. Lab.
    ATTN: G. Swinzow

Commander
US Army Comb. Arms Combat Dev. Acty.
    ATTN: LTC G. Steger
    ATTN: LTC Pullen

DEPARTMENT OF THE ARMY (Continued)

Commander
US Army Engineer Center
    ATTN: ATSEN-SY-L

Division Engineer
US Army Engineer Div. Huntsville
    ATTN: HNDED-SR

Division Engineer
US Army Engineer Div. Missouri Rvr.
    ATTN: Tech. Library

Commandant
US Army Engineer School
    ATTN: ATSE-TEA-AD
    ATTN: ATSE-CTD-CS

Director
US Army Engr. Waterways Exper. Sta.
    ATTN: Behzad Rohani
    ATTN: D. K. Butler
    ATTN: William Flathau
    ATTN: John N. Strange
    ATTN: Guy Jackson
    ATTN: Technical Library
    ATTN: P. Hadala
    ATTN: Leo Ingram

Commander
US Army Mat. & Mechanics Research Center
    ATTN: Technical Library

Commander
US Army Materiel Dev. & Readiness Command
    ATTN: Technical Library

Director
US Army Materiel Sys. Analysis Acty.
    ATTN: Joseph Sperazza

Commander
US Army Missile Command
    ATTN: F. Fleming
    ATTN: J. Hogan
    ATTN: W. Jann

Commander
US Army Mobility Equip. R & D Center
    ATTN: STSFB-XS
    ATTN: Technical Library
    ATTN: STSFB-MW

Commander
US Army Nuclear Agency
    ATTN: Doc. Con.
    ATTN: Tech. Lib.

Commander
US Army Training & Doctrine Command
    ATTN: LTC Auveduti, COL Enger
    ATTN: LTC J. Foss

Commandant
US Army War College
    ATTN: Library

US Army Mat. Cmd. Proj. Mngr. for Nuc. Munitions
    ATTN: DRCPM-NUC

DEPARTMENT OF THE NAVY

Chief of Naval Operations
Navy Department
    ATTN: Code 604C3, Robert Piacesi
    ATTN: OP 982, LCDR Smith
    ATTN: OP 982, LTC Dubac
    ATTN: OP 982 CAPT Toole

Chief of Naval Research
Navy Department
    ATTN: Technical Library

Officer in Charge
Civil Engineering Laboratory
Naval Construction Battalion Center
    ATTN: R. J. Odello
    ATTN: Technical Library

Commandant of the Marine Corps
Navy Department
    ATTN: POM

Commanding General
Development Center
Fire Support Branch
MCDEC
    ATTN: LTC Gapenski
    ATTN: CAPT Hartneady

Commander
Naval Air Systems Command
Headquarters
    ATTN: F. Marquardt

Commanding Officer
Naval Explosive Ord. Disposal Fac.
    ATTN: Code 504, Jim Petrousky

Commander
Naval Facilities Engineering Command
Headquarters
    ATTN: Technical Library

Superintendent (Code 1424)
Naval Postgraduate School
    ATTN: Code 2124, Tech. Rpts. Librarian

Director
Naval Research Laboratory
    ATTN: Code 2600, Tech. Lib.

Commander
Naval Sea Systems Command
Navy Department
    ATTN: ORD-033
    ATTN: SEA-9931G

Commander
Naval Surface Weapons Center
    ATTN: Code WA501, Navy Nuc. Prgms. Off.
    ATTN: Code WX21, Tech. Lib.
    ATTN: M. Kleinerman

Commander
Naval Surface Weapons Center
Dahlgren Laboratory
    ATTN: Technical Library

Commander
Naval Weapons Center
    ATTN: Carl Austin
    ATTN: Code 533, Tech. Lib.

DEPARTMENT OF THE NAVY

Commanding Officer
Naval Weapons Evaluation Facility
        ATTN: Technical Library

Director
Strategic Systems Project Office
Navy Department
        ATTN: NSP-43, Tech. Lib.

DEPARTMENT OF THE AIR FORCE

AF Armament Laboratory, AFSC
 3 cy ATTN: John Collins, AFATL/DLYV
        ATTN: Masey Valentine

AF Institute of Technology, AU
        ATTN: Library AFIT, Bldg. 640, Area B

AF Weapons Laboratory, AFSC
        ATTN: SUL

Headquarters
Air Force Systems Command
        ATTN: Technical Library

Commander
Armament Development & Test Center
        ATTN: Tech. Library

Assistant Secretary of the Air Force
Research & Development
Headquarters, US Air Force
        ATTN: Col R. E. Steere

Deputy Chief of Staff
Research & Development
Headquarters, US Air Force
        ATTN: Col J. L. Gilbert

Commander
Foreign Technology Division, AFSC
        ATTN: NICD, Library

Hq. USAF/IN
        ATTN: INATA

Hq. USAF/RD
        ATTN: RDPM

Oklahoma State University
Fld. Off. for Wpns. Effectiveness
        ATTN: Edward Jackett

Commander
Rome Air Development Center, AFSC
        ATTN: EMTLD, Doc. Library

SAMSO/RS
        ATTN: RSS

ENERGY RESEARCH & DEVELOPMENT ADMINISTRATION

Division of Military Application
US Energy Research & Dev. Admin.
        ATTN: Doc. Control for Test Office

ENERGY RESEARCH & DEVELOPMENT ADMINISTRATION
(Continued)

University of California
Lawrence Livermore Laboratory
        ATTN: Jerry Goudreau
        ATTN: Mark Wilkins, L-504
        ATTN: Tech. Info. Dept. L-3

Los Alamos Scientific Laboratory
        ATTN: Doc. Control for Reports Lib.
        ATTN: Doc. Control for Tom Dowler

Sandia Laboratories
Livermore Laboratory
        ATTN: Doc. Control for Tech. Library

Sandia Laboratories
        ATTN: Doc. Con. for Walter Herrmann
        ATTN: Doc. Con. for William Patterson
        ATTN: Doc. Con. for W. Altsmeifer
        ATTN: Doc. Con. for William Caudle
        ATTN: Doc. Con. for 3141 Sandia Rpt. Coll.
        ATTN: Doc. Con. for John Colp
        ATTN: Doc. Con. for John Keizur

US Energy Research & Dev. Admin.
Albuquerque Operations Office
        ATTN: Doc. Con. for Tech. Library

US Energy Research & Dev. Admin.
Division of Headquarters Services
Library Branch G-043
        ATTN: Doc. Con. for Class Tech. Lib.

US Energy Research & Dev. Admin.
Nevada Operations Office
        ATTN: Doc. Con. for Tech. Lib.

OTHER GOVERNMENT AGENCIES

NASA
Ames Research Center
        ATTN: Robert W. Jackson

Office of Nuclear Reactor Regulation
Nuclear Regulatory Commission
        ATTN: Robert Heineman
        ATTN: Lawrence Shao

DEPARTMENT OF DEFENSE CONTRACTORS

Aerospace Corporation
        ATTN: Tech. Info. Services

Agbabian Associates
        ATTN: M. Agbabian

Applied Theory, Inc.
 2 cy ATTN: John G. Trulio

Avco Research & Systems Group
        ATTN: David Henderson
        ATTN: Research Lib. A830, Rm. 7201
        ATTN: Pat Grady
        ATTN: Samuel Skemp

Battelle Memorial Institute
        ATTN: Technical Library

DEPARTMENT OF DEFENSE CONTRACTORS (Continued)

The BDM Corporation
    ATTN: Technical Library

The Boeing Company
    ATTN: Aerospace Library

California Research & Technology, Inc.
    ATTN: Technical Library
    ATTN: Ken Kreyenhagen

Civil/Nuclear Systems Corp.
    ATTN: Robert Crawford

EG&G, Inc.
Albuquerque Division
    ATTN: Technical Library

Engineering Societies Library
    ATTN: Ann Mott

General Dynamics Corp.
Pomona Division
    ATTN: Keith Anderson

General Electric Company
TEMPO-Center for Advanced Studies
    ATTN: DASIAC

Georgia Institute of Technology
Georgia Tech. Research Institute
    ATTN: S. V. Hanagud
    ATTN: L. W. Rehfield

Honeywell Incorporated
Defense Systems Division
    ATTN: T. N. Helvig

Institute for Defense Analyses
    ATTN: IDA Librarian, Ruth S. Smith

Kaman AviDyne
Division of Kaman Sciences Corp.
    ATTN: E. S. Criscione
    ATTN: Norman P. Hobbs
    ATTN: Technical Library

Kaman Sciences Corporation
    ATTN: Library

Lockheed Missiles & Space Company, Inc.
    ATTN: M. Culp
    ATTN: Technical Library

Lockheed Missiles & Space Company, Inc.
    ATTN: Tech. Info. Center D/Coll.

Martin Marietta Aerospace
Orlando Division
    ATTN: H. McQuaig
    ATTN: Al Cowen
    ATTN: M. Anthony

Merritt Cases, Incorporated
    ATTN: Technical Library
    ATTN: J. L. Merritt

University of New Mexico
Dept. of Campus Security & Police
    ATTN: G. E. Triandafalidis

Nathan M. Newmark
Consulting Engineering Services
    ATTN: Nathan M. Newmark

Pacifica Technology
    ATTN: R. Bjork
    ATTN: G. Kent

Physics International Company
    ATTN: Doc. Con. for Larry A. Behrmann
    ATTN: Doc. Con. for Dennis Orphal
    ATTN: Doc. Con. for Charles Godfrey
    ATTN: Doc. Con. for Tech. Lib.

R & D Associates
    ATTN: William B. Wright, Jr.
    ATTN: Harold L. Brode
    ATTN: Technical Library
    ATTN: Paul Rausch
    ATTN: Henry Cooper
    ATTN: Cyrus P. Knowles
    ATTN: Arlen Fields
    ATTN: J. G. Lewis

The Rand Corporation
    ATTN: Technical Library

Science Applications, Inc.
    ATTN: Technical Library

Stanford Research Institute
    ATTN: George R. Abrahamson
    ATTN: Jim Colton

Systems, Science & Software, Inc.
    ATTN: Robert Sedgewick
    ATTN: Technical Library

Terra Tek, Inc.
    ATTN: Technical Library

TRW Defense & Space Sys. Group
    ATTN: Peter K. Dai, R1/2170
    ATTN: Tech. Info. Center/S-1930

TRW Defense & Space Sys. Group
San Bernardino Operations
    ATTN: E. Y. Wong, 527/712

Weidlinger Assoc. Consulting Engineers
    ATTN: Melvin L. Baron
    ATTN: J. M. McCormick

Weidlinger Assoc. Consulting Engineers
    ATTN: J. Isenberg